الشعبية الديمقراطية الجزائرية الجمهورية

Algerian Democratic and Popular Republic

العلمي والبحث العالي التعليم وزارة

Ministry of Higher Education and Scientific Research

ورقلة – مرباح قاصدي جامعة

Kasdi Merbah University – Ouargla

Faculty of Applied Sciences and Technology

Department of Mechanical Engineering

END OF STUDIES THESIS

For the award of the Master 2 degree in

Mechanical Engineering — Specialty: Manufacturing Engineering

Génie Mécanique Spécialité : Fabrication Mécanique

Modeling and Optimization of Machining Parameters during Dry Turning of AISI 316L Stainless Steel

PRESENTED BY :
BENGADI RABEH
DOUNANE MOHAMMED SIF ALLAH

SUPERVISORED BY :
DR. YOUSSEF TOUGGUI

Evaluation Jury:

Nam	Role
Dr. BOUAkBA MUSTAfA	President
Dr. AMEUR TOUFIK	Examiner

Academic Year: 2025–2026

Dedication

To my beloved family, whose endless patience, encouragement, and sacrifices made every page of this thesis possible.

To my supervisor, for guiding this work with expertise and dedication.

To my friends and colleagues, whose support sustained me through the challenges of this research.

To all those who believe in the value of knowledge

Acknowledgements

First and foremost, we would like to express our sincere gratitude to my thesis supervisor, Dr.Youssef Touggui for his invaluable guidance, expert advice, continuous support, and patience throughout this research. his deep knowledge and rigorous scientific approach have been a constant source of inspiration.

we also extend our warm thanks to the members of the jury for accepting to evaluate this thesis and for the time and effort they have dedicated to reading and assessing this work.

We are grateful to the professors and staff of the Department of Mechanical Engineering (Fabrication Mécanique) at the University of Kasdi Merbah Ouargla, whose excellent teaching established the academic foundation upon which this research is built.

Special thanks go to our colleagues and fellow students for the helpful discussions, shared resources, and moral support throughout the course of this Master program.

Finally, our deepest and most heartfelt thanks go to our famillies, whose love, encouragement, and unwavering belief in me have been our greatest strength throughout this journey.

Abstract

This thesis presents a comprehensive study on the modeling and optimization of turning parameters for AISI 316L austenitic stainless steel a material of major industrial importance widely used in biomedical, chemical, and marine applications. Three input parameters are investigated: cutting speed (Vc), feed rate (f), and depth of cut (ap), each at three levels, organized using a Taguchi L27 orthogonal array comprising 27 experimental runs. The two measured output responses are surface roughness (Ra) and tangential cutting force (Fz). Response Surface Methodology (RSM) is applied to develop second order polynomial predictive models for both responses using Design Expert 10 software. Analysis of Variance (ANOVA) is performed to evaluate the statistical significance and percentage contribution of each factor and their interactions.

Multi objective optimization is carried out using the Desirability Function, which simultaneously minimizes both Ra and Fz.

Keywords: AISI 316L stainless steel, turning, surface roughness, cutting force

Résumé

Ce mémoire présente une étude complète sur la modélisation et l'optimisation des paramètres de tournage de l'acier inoxydable austénitique AISI 316L un matériau d'importance industrielle majeure, largement utilisé dans les applications biomédicales, chimiques et marines. Trois paramètres d'entrée sont étudiés : la vitesse de coupe (Vc), l'avance (f) et la profondeur de passe (ap), chacun à trois niveaux, organisés selon le plan d'expériences orthogonal Taguchi L27 comprenant 27 essais expérimentaux. Les deux réponses mesurées sont la rugosité de surface Ra et la force de coupe tangentielle Fz. La Méthode des Surfaces de Réponse (RSM) est appliquée pour développer des modèles de prédiction polynomiaux du second ordre pour les deux réponses, en utilisant le logiciel Design Expert 10. L'analyse de la variance (ANOVA) permet d'évaluer la signification statistique et le pourcentage de contribution de chaque facteur.

L'optimisation multi objectif est réalisée par la Fonction de Désirabilité.

Mots clés : Acier inoxydable AISI 316L , tournage, rugosité de surface , force de coupe

ملخص

تقدم هذه المذكرة دراسة حول نمذجة وتحسين معاملات الخراطة للفولاذ المقاوم للصدأ الأوستنيتي AISI 316L، وهو مادة ذات أهمية صناعية كبرى وتُستخدم على نطاق واسع في التطبيقات الطبية الحيوية، والكيميائية، والبحرية. جرى استقصاء ثلاثة معاملات مدخلة هي: سرعة القطع (Vc)، ومعدل التغذية (f)، وعمق القطع (ap)، بحيث يشمل كل منها ثلاثة مستويات، وتم تنظيمها باستخدام مصفوفة تاغوتشي التعامدة L27 التي تضم 27 شوطاً تجريبياً. تمثلت الاستجابات المخرجة المقاسة في خشونة السطح (Ra) وقوى القطع المماسية (Fz). جرى تطبيق منهجية سطح الاستجابة (RSM) لتطوير نماذج تنبؤية متعددة الحدود من الدرجة الثانية لكلتا المخرجتين باستخدام برنامج Design Expert 10. كما تم إجراء تحليل التباين (ANOVA) لتقييم الأهمية الإحصائية ونسبة مساهمة كل عامل والتفاعلات بينها.

جرى إجراء تحسين متعدد الأهداف باستخدام دالة المرغوبية، والتي تقلل من Ra و Fz في آن واحد.

الكلمات المفتاحية: الفولاذ المقاوم للصدأ AISI 316L، الخراطة، خشونة السطح، قوى القطع

Table of Contents

List of Figures

List of Tables

Nomenclature

Symbol	Description / Unit
ANOVA	Analysis of Variance
ap	Depth of cut (mm)
BUE	Built Up Edge
C.V.%	Coefficient of Variation (%)
CNC	Computer Numerical Control
D	Workpiece diameter (mm)
DF	Desirability Function
df	Degrees of freedom
DoE	Design of Experiments
f	Feed rate (mm/rev)
F	Fisher's F ratio statistic
Fz	Tangential cutting force (N)
GA	Genetic Algorithm
MRR	Material Removal Rate (mm^3/min)
MS	Mean Square (SS/df)
N	Spindle rotational speed (rpm)
p	Probability value (Prob > F)
PVD	Physical Vapour Deposition
R^2	Coefficient of Determination
Ra	Arithmetic mean surface roughness (µm)
RSM	Response Surface Methodology
Rth	Theoretical peak to valley roughness (mm)
rε	Tool nose radius (mm)
S/N	Signal to Noise ratio (dB)
SA	Simulated Annealing
SS	Sum of Squares
TiAlN	Titanium Aluminium Nitride
TiCN	Titanium Carbo Nitride
Vc	Cutting speed (m/min)
β_0	Model intercept coefficient
β_i	Linear regression coefficient for factor i
β_{ii}	Quadratic regression coefficient for factor i
β_{ij}	Interaction regression coefficient for factors i and j

General Introduction

The machining industry is a cornerstone of modern manufacturing, converting raw material into precision components for a wide range of sectors from aerospace and automotive to biomedical engineering and chemical processing. Among the many machining operations, turning is one of the most widely practised, used to produce cylindrical parts to precise dimensional and surface quality specifications. The ability to control and optimize the parameters governing this process is therefore of fundamental technological and economic importance.

The three primary input parameters in a turning operation are cutting speed (Vc), feed rate (f), and depth of cut (ap). These parameters jointly determine the material removal rate, the surface quality of the finished part, the cutting forces acting on the tool and workpiece, and the tool wear rate. Selecting them correctly produces high quality parts at low cost with extended tool life. Selecting them poorly results in high surface roughness, excessive cutting forces, rapid tool wear, increased energy consumption, and high production costs.

Among the wide range of engineering materials used in industry, AISI 316L austenitic stainless steel occupies a position of particular importance. Its exceptional corrosion resistance, and mechanical strength make it the preferred material for biomedical implants, surgical instruments, chemical reactors, marine hardware, and nuclear components. However, it is also classified as a difficult to machine material due to its low thermal conductivity, strong work , and susceptibility to built up edge formation characteristics that make the optimal selection of turning parameters especially critical and challenging.

In this context, systematic experimental design methods and mathematical modeling techniques provide the tools needed to efficiently characterize and optimize the turning process. The Taguchi L27 orthogonal array allows a three factor, three level study to be conducted with only 27 carefully balanced experimental runs. Response Surface Methodology (RSM) then fits a quadratic polynomial model to the experimental results, enabling the construction of three dimensional response surfaces that reveal how each parameter and their interactions influence the output responses. Analysis of Variance (ANOVA) provides the statistical framework to quantify the relative contribution of each factor, while the Desirability Function translates multi objective optimization into a single composite criterion that can be maximized numerically.

The present thesis applies this combined Taguchi RSM Desirability Function framework to the dry turning of AISI 316L stainless steel using a Sandvik cermet insert (GC1525). The specific objectives are to study the individual and combined effects of Vc, f, and ap on surface roughness Ra and tangential cutting force Fz , to develop and validate RSM quadratic prediction models for both responses , to determine the statistical significance and percentage contribution of each factor using ANOVA ,and to identify the optimal cutting conditions that simultaneously minimize Ra and Fz using the Desirability Function.

To achieve these objectives, the thesis is organised into three chapters. Chapter I provides a comprehensive literature review covering the fundamental aspects of the turning process, the cutting parameters and output responses under study, and a critical survey of published works on the machinability of austenitic stainless steels, the application of Taguchi design and RSM, predictive modeling techniques including artificial neural networks, and desirability-based multi-objective optimization. Chapter II presents the mathematical modeling and optimization methodology, detailing the RSM quadratic model development, the derived predictive equations for Ra and Fz, and the application of the Desirability Function to identify optimal cutting conditions. Chapter III discusses the experimental results and model outcomes, the ANOVA-based statistical analysis of factor contributions presenting response surface and contour plot analyses, validating the RSM predictive models against experimental data, and situating the optimized cutting conditions within the context of the open literature.

CHAPTER I

Literature Review

I.1 Introduction

Turning is one of the most widely used metal cutting operations in the manufacturing industry. The quality of a turned part depends directly on the selection of cutting parameters. Choosing incorrect parameters leads to poor surface finish, excessive cutting forces, accelerated tool wear, and increased production costs. To avoid these problems, researchers have developed systematic methods to model the relationships between cutting conditions and measurable output responses, and then to optimize those conditions for the best possible results.

This chapter presents the theoretical foundation and state of the art required for this research. It defines the turning process and its fundamental input parameters, explains the output responses under study surface roughness (Ra) and cutting force (Fz) and reviews recent published work on the modeling and optimization of turning operations. The review covers a range of workpiece materials and methodological approaches, including the Taguchi method, Response Surface Methodology (RSM), Analysis of Variance (ANOVA), and computational optimization techniques such as Genetic Algorithms (GA) and Artificial Neural Networks (ANN). The chapter closes with an identification of the research gap that this thesis aims to address.

I.2 The Turning Process

Turning is a material removal process in which a single point cutting tool removes material from a rotating cylindrical workpiece to produce a finished part of the desired geometry and surface quality. The workpiece is held in a chuck and rotates at a controlled spindle speed, while the tool moves linearly along the workpiece axis. The machine tool used is a lathe conventional or CNC. In industrial and research settings, CNC lathes are preferred because they allow precise and repeatable control of all cutting parameters.

The cutting tool in turning is typically a carbide insert mounted on a tool holder. The insert geometry nose radius, rake angle, and clearance angle directly influences the cutting forces and the surface finish. In industrial practice, coated carbide and cermet inserts are the most common choices. Touggui [1] compared cermet (GC1525) and coated carbide (GC1125) inserts in the dry turning of AISI 316L stainless steel, demonstrating the significant influence of insert type on both Ra and Fz.

During turning, three basic cutting motions occur simultaneously: the primary cutting motion (rotation of the workpiece), the feed motion (linear movement of the tool along the axis), and the depth setting motion (radial positioning of the tool). These three motions correspond directly to the three fundamental input parameters: cutting speed, feed rate, and depth of cut.

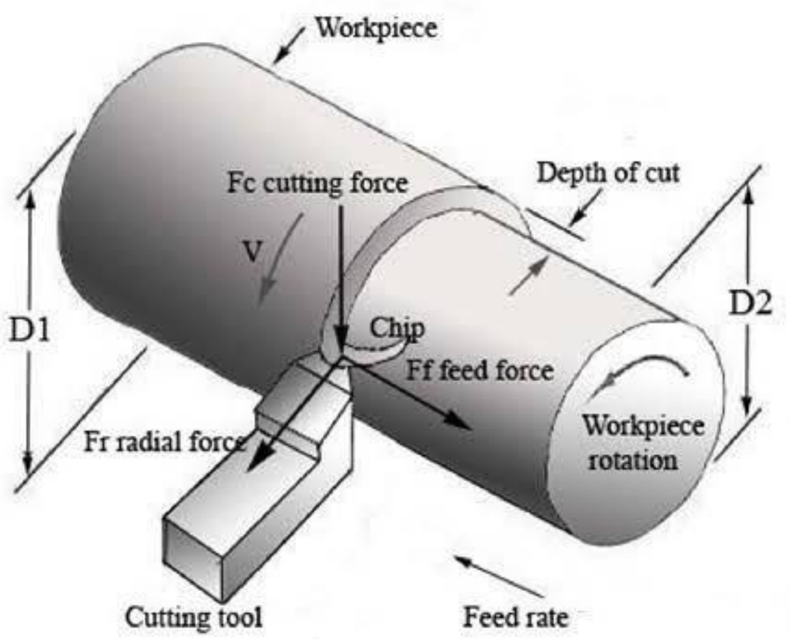

Figure I.3 : Schematic diagram of the turning operation

I.3 Fundamental Cutting Parameters

I.3.1 Cutting Speed (Vc)

Cutting speed is the linear velocity at the surface of the workpiece at the point of cutting contact, expressed in meters per minute (m/min). It is related to the spindle rotational speed N (rpm) and workpiece diameter D (mm) by:

$$\boldsymbol{Vc = (\pi \times D \times N) / 1000} \quad [\boldsymbol{m/min}] \qquad (\mathbf{1})$$

Higher cutting speeds generally reduce contact time between tool and chip, lower cutting forces, and can improve surface finish. However, excessively high speeds accelerate tool wear due to elevated temperatures at the cutting zone. For difficult to machine materials such as AISI 316L, cutting speed must be carefully balanced against productivity and tool life [1].

I.3.2 Feed Rate (f)

Feed rate is the distance the cutting tool advances along the workpiece per revolution of the spindle, expressed in mm/rev. It has the strongest direct influence on surface roughness through the geometry of feed marks left on the machined surface. [1].

I.3.3 Depth of Cut (ap)

Depth of cut is the radial distance over which the cutting tool engages the workpiece in a single pass (mm). It directly controls the chip cross sectional area and therefore has the greatest influence on cutting forces. Research by DR.Touggui . [1] found that depth of cut accounted for 62.1% of the variation in Fz for cermet inserts on AISI 316L. It is also the primary lever for controlling material removal rate and machining productivity.

I.4 Output Responses

I.4.1 Surface Roughness (Ra)

The arithmetic mean roughness Ra is the most commonly used surface texture parameter. It represents the average absolute deviation of the surface profile from the mean line over the evaluation length, measured in micrometers (μm) by a contact profilometer following ISO 4287. Ra is a critical quality indicator: high roughness increases friction, accelerates wear, and reduces fatigue life in mechanical components. In biomedical applications it affects corrosion resistance and tissue integration. Minimizing Ra is therefore a primary optimization objective in turning studies [1].

In turning, Ra is primarily controlled by feed rate and nose radius. However, vibration, built up edge (BUE) formation, and material work hardening can also degrade surface quality independently of the geometry based prediction. These additional effects are particularly relevant when machining austenitic stainless steels.

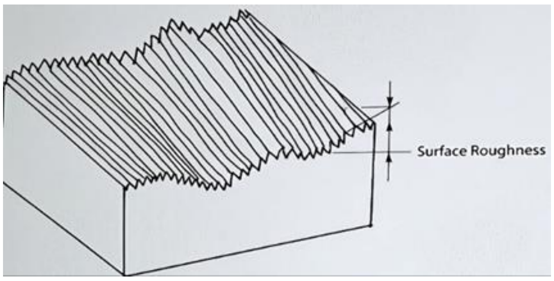

Figure I.4 : Surface roughness Ra profile definition

I.4.2 Tangential Cutting Force (Fz)

The tangential cutting force Fz is the dominant component of the resultant cutting force, acting opposite to the direction of workpiece rotation. It is directly responsible for spindle torque, power consumption, elastic deflection of the tool workpiece system, and heat generation at the cutting zone. Reducing Fz brings multiple benefits: lower energy costs, extended tool life, and improved dimensional accuracy especially important for slender workpieces or thin walled components. Fz increases with depth of cut and feed rate due to the enlarged chip cross section, while cutting speed has a secondary and often inverse effect through thermal softening [1]

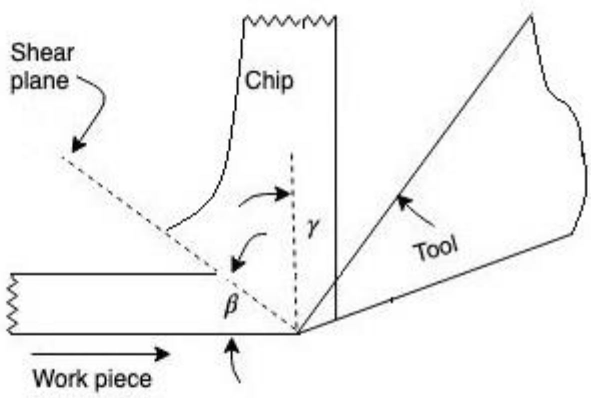

Figure I.5 : Chip formation mechanism in turning

I.5 Literature Review: State of the Art

I.5.1 Machinability of Austenitic Stainless Steels: An Overview

Austenitic stainless steels, owing to their outstanding combination of corrosion resistance, ductility, and elevated temperature performance, occupy a central role in demanding industrial sectors including biomedical engineering, chemical processing, and marine applications. Their machinability, however, is widely recognized as challenging due to three intrinsic characteristics: low thermal conductivity, which concentrates heat at the tool–chip interface, a pronounced work hardening tendency, which progressively hardens the subsurface layer ahead of the cutting edge , and a high susceptibility to built up edge (BUE) formation at moderate cutting speeds, which destabilizes the cutting forces and deteriorates surface integrity [2].

Several investigations have specifically addressed these machinability issues. Kaladhar . [2] provided a comprehensive review of the machining of austenitic stainless steels, systematically identifying the dominant mechanisms of tool wear and surface quality degradation, and establishing that low thermal conductivity combined with high work hardening propensity are the primary barriers to productive machining. In the context of tool selection for these materials, Kaladhar [3] subsequently evaluated the performance of multiple hard coating materials during turning operations and demonstrated that the type and architecture of the insert coating exert a decisive influence on surface roughness and material removal rate a finding of direct relevance to the selection of a PVD coated cermet insert for the present study.

Further evidence of the machinability challenges associated with austenitic grades comes from drilling studies conducted on related alloys. Nomani . [4] compared the machinability of AISI 2507 duplex, AISI 2205 duplex, and AISI 316L austenitic stainless steel in terms of tool wear, cutting forces, and surface finish, and concluded that AISI 316L exhibited relatively superior machinability among the three grades investigated. This comparative finding contextualizes the choice of AISI 316L as the workpiece material in the present thesis while underscoring that it remains a difficult to machine material in absolute terms.

At the tool material interface, Patel . [5] investigated the behavior of cermet inserts during high speed dry finish turning of AISI 304 austenitic stainless steel, focusing on the influence of secondary carbides within the cermet microstructure on wear mechanisms and cutting performance. Their findings confirmed that PVD coated cermet inserts offer effective resistance to the diffusion and adhesion wear mechanisms that dominate when machining austenitic stainless steels under dry conditions directly supporting the rationale for using the Sandvik GC1525 cermet insert (CNMG 120408 PF) in the present work.

Figure I.4 :AISI 316L austenitic stainless steel microstructure

I.5.2 Experimental Design: Taguchi Method and Response Surface Methodology

The Taguchi method, based on orthogonal arrays, has become the de facto standard for structured experimental design in turning research. By assigning factor levels in a mathematically balanced manner, orthogonal arrays allow the independent estimation of main effects from a compact experimental plan. Kaladhar [6] applied the Taguchi method combined with ANOVA to determine the optimum cutting parameters during the turning of AISI 304 austenitic stainless steel, confirming the effectiveness of this approach for stainless steel machining and establishing benchmark results against which subsequent studies are evaluated.

Response Surface Methodology (RSM) extends the Taguchi approach by fitting a continuous polynomial model to the experimental data. The second order quadratic model captures both linear effects and curvature, and is particularly well suited to the non linear relationships between cutting parameters and measured responses that are characteristic of metal cutting processes[07]. Berkani [08] employed RSM to model surface roughness and cutting force during the turning of AISI 304 stainless steel using a CVD coated carbide insert, obtaining coefficient of determination values of $R^2 = 96.84\%$ and $R^2 = 99.61\%$ for the surface roughness and force models, respectively. Bagaber and Yousof [8] also constructed an RSM model for surface roughness during the turning of AISI 316 stainless steel, reporting an R^2 value of 93.5% a result in good agreement with the Ra model quality achieved in the present study ($R^2 = 90.65\%$). These published benchmarks confirm that an R^2 in the range of 90–97% is typical for RSM based surface roughness models in the turning of stainless steels, while cutting force models consistently exceed 99%.

Sarikaya [9] combined signal to noise analysis, RSM, and regression based approaches for the optimization of process parameters in micro electrical discharge machining of AISI 304, demonstrating the versatility of the Taguchi–RSM framework across different machining processes and materials A. K. Gupta. [10] applied RSM to simultaneously optimize surface roughness and material removal rate during the turning of X20Cr13 stainless steel, achieving a fully characterized response surface that enabled direct identification of the Pareto front between productivity and surface quality an approach conceptually aligned with the desirability function based multi objective optimization performed in the present thesis.

I.5.3 Predictive Modeling: RSM versus Artificial Neural Networks

A growing body of literature has compared RSM and Artificial Neural Network (ANN) approaches for predicting surface roughness and cutting forces in turning operations. The general finding across these studies is that ANN models provide marginally superior predictive accuracy over RSM quadratic models, particularly for surface roughness, while both approaches deliver acceptable performance for cutting force prediction.

Laouissi . [11] conducted a systematic comparison of RSM and ANN models for predicting surface roughness and tangential cutting force during the turning of X210Cr12 steel under dry and other cutting conditions, incorporating cutting speed, feed rate, depth of cut, and nose radius as input variables. Their experimental results demonstrated that ANN trained models yielded more precise predictions than RSM for both responses a finding that motivated the inclusion of an ANN analysis as a complementary modeling technique in the present work. Laouissi . [11] presented an analogous comparative study for the turning of gray cast iron using ceramic tools, evaluating model accuracy through mean absolute deviation (MAD), mean absolute percentage error (MAPE), root mean square error (RMSE), and coefficient of determination (R^2). They reported MAPE values for Ra and Fz varying between 1.95% and 9.30% across models, and consistently concluded that ANN outperformed RSM in predictive accuracy.

Tebassi . [12] applied both ANN and RSM to predict surface roughness and tangential cutting force during the turning of Inconel 718 superalloy, reporting R^2 values of 0.93 and 0.98 for the RSM models and 0.98 and 0.99 for the ANN models of Ra and Fz, respectively. The pattern ANN slightly superior to RSM is consistent across all three studies. Gupta [14] extended this comparison to include support vector regression (SVR) in addition to RSM and ANN for the prediction of surface roughness during the turning of a metal matrix composite, and concluded that ANN was the most robust of the three approaches.

Of particular relevance to the present study is the work of Acayaba and Muñoz de Escalona [15], who developed predictive models of surface roughness specifically during the turning of AISI 316L austenitic stainless steel at low cutting speeds using multiple linear regression and ANN. Their study provided the first systematic predictive model for this exact material, establishing baseline Ra values and identifying the dominant influence of feed rate a finding fully consistent with the 78.25% feed rate contribution to Ra documented in the present work. Similarly, Kara . [16] developed ANN based models for predicting cutting forces in the orthogonal turning of AISI 316L, comparing performance metrics on training and testing datasets and demonstrating that the ANN achieved excellent agreement with experimental measurements.

Nur . [17] also studied the machinability of AISI 316L stainless steel specifically with coated carbide tools, analyzing the influence of machining parameters on cutting forces and surface roughness and providing quantitative data relevant to the selection of cutting conditions in the present experimental plan.

I.5.4 Optimization Techniques: the Desirability Function

The Desirability Function (DF) is one of the most commonly used optimization techniques in machining processes, particularly for multi-response optimization problems. This approach converts each response into an individual desirability value ranging from 0 to 1, where a value closer to 1 indicates a more desirable outcome. The individual desirability values are then combined into a single composite desirability index, enabling the determination of machining conditions that simultaneously satisfy multiple objectives. Due to its simplicity, effectiveness, and compatibility with Response Surface Methodology (RSM), the Desirability Function has been widely adopted in turning optimization studies.

Bagaber and Yousof [7] applied the Desirability Function to optimize the turning of AISI 316 stainless steel by simultaneously minimizing surface roughness and energy-related responses. The optimized machining parameters resulted in a reduction of surface roughness by 4.71% compared with the baseline conditions, demonstrating the effectiveness of the DF approach in achieving improved machining performance while considering multiple objectives.

In another study, Berkani [8]. employed the Desirability Function for the optimization of turning parameters during the machining of AISI 304 stainless steel. The objective was to simultaneously minimize tangential cutting force and surface roughness. The optimal solution was obtained at a depth of cut of 0.295 mm, a cutting speed of 104.54 m/min, and a feed rate of 0.08 mm/rev. The results confirmed the capability of the Desirability Function to identify machining conditions that provide a suitable compromise between productivity and surface quality.

Mia and Dhar [18] also demonstrated the applicability of the Desirability Function in hard turning operations. Their optimization study indicated that lower feed rates combined with higher cutting speeds produced improved surface finish, confirming the sensitivity of surface roughness to cutting parameters and highlighting the usefulness of DF in determining optimal machining settings.

Furthermore, Zerti et al. conducted a comprehensive multi-objective optimization study on the turning of AISI 420 tempered stainless steel. Surface roughness, cutting force, and power consumption were minimized while productivity was maximized using a desirability-based optimization strategy. The authors concluded that the integration of RSM predictive models with the Desirability Function constitutes a robust and computationally efficient framework for solving complex machining optimization problems.

Based on the findings reported in the literature, the Desirability Function can be considered a reliable and effective optimization technique for turning processes. Its ability to simultaneously optimize multiple performance characteristics through a single objective function makes it particularly suitable for machining applications where quality, productivity, and energy efficiency must be balanced. Consequently, the Desirability Function was selected in the present study as the optimization tool for determining the optimal cutting conditions for the turning of AISI 316L stainless steel.

I.5.5 The Dominant Role of Feed Rate on Surface Roughness

The pre eminence of feed rate as the controlling factor for surface roughness in turning is one of the most consistently reproduced findings in the machining literature, confirmed across a broad range of workpiece materials and tool types. This dominance has a firm theoretical basis: the geometry of feed marks left on the machined surface produces a surface texture whose amplitude scales directly with feed rate and nose radius. In the turning of austenitic stainless steels specifically, the role of feed rate is amplified by the tendency of the material to generate BUE at low cutting speeds, which introduces additional surface damage that is superimposed on the geometric feed mark pattern.

Quantitative evidence from the studies reviewed confirms this pattern. Kaladhar found feed rate to be the dominant contributor to Ra in the turning of AISI 304 stainless steel regardless of insert type. Berkani [2] similarly identified feed rate as the primary Ra driver in turning of AISI 304 stainless steel with a CVD coated carbide tool. Acayaba and Muñoz de Escalona working specifically on AISI 316L, confirmed that feed rate governed surface roughness in the low speed turning regime. In the present study, feed rate accounts for 78.25% of total Ra variation ($F = 142.28$, $p < 0.0001$), a result in quantitative agreement with the 79.61% contribution reported by the primary reference for this experimental dataset [19].

I.5.6 Depth of Cut as the Primary Driver of Cutting Force

The analytical literature is equally consistent in identifying depth of cut as the dominant factor governing tangential cutting force Fz. The physical mechanism is direct: depth of cut controls the chip cross sectional area (together with feed rate), and Fz scales linearly with chip area through the specific cutting pressure. An increase in ap therefore produces a proportional increase in the material volume removed per unit time and, consequently, in the cutting force.

Berkani . [2] confirmed the dominant role of depth of cut for cutting force in the turning of AISI 304. Bouacha . [3] demonstrated the same pattern in the hard turning of bearing steel using cubic boron nitride (CBN) tools, reporting that depth of cut was consistently the most influential factor on all force components across the studied parameter space. In the present study, depth of cut contributes 60.24% to total Fz variation, followed by feed rate at 35.42% a result in near perfect agreement with the 62.12% contribution of ap and 35.23% contribution of f reported for the cermet insert in the primary reference study [19]. The residual experimental error is only 0.32%, which explains the exceptional coefficient of determination ($R^2 = 0.9968$) of the Fz predictive model.

I.5.7 Performance of Cermet Inserts in the Turning of Stainless Steels

The selection of cutting insert material and coating is a critical factor in determining machinability outcomes when turning difficult to machine materials such as AISI 316L. Cermet inserts composite materials combining hard ceramic particles (primarily titanium carbide, TiC) with a metallic binder are particularly suited to finish turning operations where smooth surfaces and low cutting forces are required. Their resistance to crater wear and lower chemical affinity for iron based alloys compared to cemented carbide makes them advantageous for the turning of austenitic stainless steels.

Kaladhar [3] evaluated multiple hard coating architectures applied to cermet and carbide substrates during the turning of AISI 304 stainless steel and found that TiCN–TiN PVD coated cermet inserts produced competitive surface quality comparable to the best TiAlN–TiN coated carbide inserts, while offering superior thermal stability. Patel . [5] specifically investigated

TiCN–TiN PVD cermet inserts (the same coating architecture as the GC1525 insert used in the present thesis) during dry finish turning of AISI 304, and attributed the performance of these inserts to their resistance to the adhesion and diffusion wear mechanisms that dominate at the tool–chip interface when machining austenitic stainless steels without coolant. These published findings directly validate the selection of the Sandvik GC1525 (CNMG 120408 PF) cermet insert as the cutting tool for the present experimental campaign.

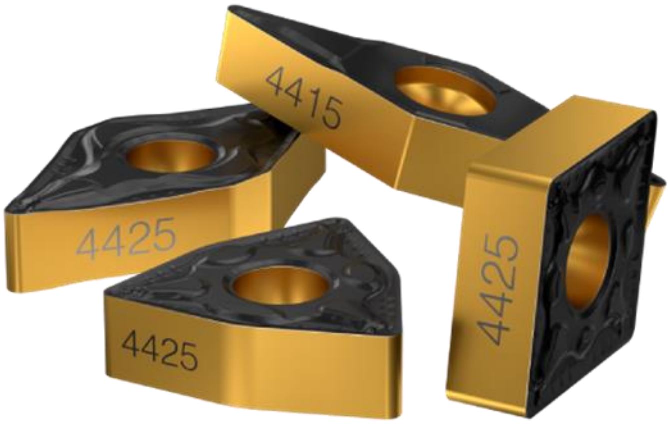

Figure I.5 Sandvik CNMG inserts: GC1525 cermet

I.5.8 Summary of Reviewed Studies and Identified Research Gap

Table 1.1 summarizes the key characteristics and findings of the principal works reviewed in this section, providing a structured basis for identifying the research gap addressed by the present thesis.

Author(s) & Year	Material / Process	Method(s)	Optimization	Key Finding
Kaladhar . (2012) [2]	AISI 304 – Turning	Taguchi + ANOVA	Parameter ranking	Feed rate dominant for Ra, LTC & thermal conductivity govern tool wear
Kaladhar (2019) [6]	AISI 304 – Turning	Experimental	Insert comparison	TiCN–TiN cermet competitive with TiAlN–TiN carbide for surface quality
Patel . (2020) [5]	AISI 304 – Dry Turning	Experimental	Wear analysis	PVD cermet resists adhesion/diffusion wear in stainless steel dry turning
Kara . (2014) [14]	AISI 316L – Orthogonal Turning	ANN	Force prediction	ANN achieves high accuracy for Fz prediction in AISI 316L turning
Nouioua . (2017) [03]	X210Cr12 – Turning	RSM + ANN	Comparative modeling	ANN more precise than RSM for both Ra and Fz prediction
Laouissi . (2019) [11]	Gray Iron – Turning	RSM + ANN + GA	Multi objective GA	ANN > RSM, MAPE 1.95–9.30%, GA optimizes f in 0.08–0.12 mm/rev range

Author(s) & Year	Material / Process	Method(s)	Optimization	Key Finding
Tebassi . (2017) [12]	Inconel 718 – Turning	RSM + ANN	Comparative modeling	ANN: R^2=0.98/0.99, RSM: R^2=0.93/0.98 for Ra/Fz
Berkani . (2015) [08]	AISI 304 – Turning (CVD)	RSM + DF	Desirability Function	Optimal: ap=0.295 mm, Vc=104 m/min, f=0.08 mm/rev, R^2=96.84%/99.61%
Bagaber & Yousof (2017) [07]	AISI 316 – Turning	RSM + DF	Multi objective DF	Ra reduced by 4.71% at optimal cutting parameters, R^2=93.5% for Ra
Zain . (2011) [19]	Abrasive Waterjet	GA + SA	Comparative optimization	GA converges faster than SA, both deliver satisfactory optima
Mia & Dhar (2017, 2018) [16,17]	Hard Turning	RSM + SA + GA + DF	Single objective	SA/GA/DF converge to similar optima, GA preferred for speed
Zerti . (2019) [18]	AISI 420 – Turning	RSM + DF	Multi objective DF	Simultaneous minimization of Ra, Fz, Power with R^2>96%

Table I.1 Summary of reviewed studies on the turning of austenitic stainless steels and related materials

The review conducted above reveals a consistent body of knowledge: feed rate is the dominant factor for surface roughness across all workpiece materials and tool types examined, depth of cut governs cutting force, the Taguchi–RSM–Desirability Function framework is well established and validated for three factor turning optimization, and ANN models provide marginally higher predictive accuracy than RSM but at the cost of significantly greater model complexity and a loss of the explicit analytical equation form provided by RSM. While individual studies address Ra and Fz separately or investigate different stainless steel grades, a comprehensive and simultaneous treatment of both responses under a Taguchi L27 plan with full ANOVA contribution quantification, RSM modeling, ANN comparative analysis, and multi objective Desirability Function optimization, applied specifically to the dry turning of AISI 316L with a PVD coated cermet insert, has not been fully established in a single integrated study. The present thesis addresses this gap directly.

I.6 Conclusion

This chapter presented the theoretical framework and state of the art for this research. The turning process was described with its three input parameters (Vc, f, ap) and two output responses (Ra and Fz). The literature unambiguously confirms that feed rate dominates Ra and depth of cut governs Fz across all materials and tool types reviewed.

CHAPTER II

Mathematical Modeling and Optimization

II.1 Introduction

The experimental data collected from the 27 Taguchi L27 runs described in Chapter 2 form the basis for the work presented in this chapter. The objectives are threefold: (1) to build accurate RSM mathematical models relating Vc, f, and ap to Ra and Fz, (2) to analyze the statistical significance and relative contribution of each factor using ANOVA, and (3) to identify the optimal cutting conditions that simultaneously minimize Ra and Fz using the Desirability Function implemented in Design Expert 10.0.1.

All modeling and analysis used a Response Surface study type with a User Defined 27 run design and a Quadratic model order applied to both responses under no data transformation ($\lambda = 1$), confirmed as appropriate by Box Cox analysis given response ratios of 3.44 for Ra and 5.69 for Fz both below the transformation threshold of 10.

II.2 Experimental Results

Table III.1 presents the complete 27 experimental results. Ra ranged from 0.43 µm (Run 2: Vc=125, f=0.08, ap=0.2) to 1.48 µm (Run 9: Vc=125, f=0.16, ap=0.3) a 3.44 fold range. Fz ranged from 23.84 N (Run 1) to 135.72 N (Run 27) a 5.69 fold range. Feed rate clearly controls Ra: all nine Ra values at f=0.08 are below 0.88 µm, while all at f=0.16 exceed 1.17 µm. Depth of cut and feed rate jointly drive Fz upward, while cutting speed shows a secondary and smaller effect on both responses.

Table II.1 Experimental results: L27 design with measured Ra and Fz values

Run	Vc (m/min)	f (mm/rev)	ap (mm)	Ra (µm)	Fz (N)
1	125	0.08	0.1	0.88	23.84
2	125	0.08	0.2	0.43	56.27
3	125	0.08	0.3	0.81	77
4	125	0.12	0.1	1.19	46.8
5	125	0.12	0.2	0.68	80.1
6	125	0.12	0.3	1.19	110
7	125	0.16	0.1	1.41	55.65
8	125	0.16	0.2	1.42	98.99
9	125	0.16	0.3	1.48	128.6
10	170	0.08	0.1	0.51	26
11	170	0.08	0.2	0.51	55.9

Run	Vc (m/min)	f (mm/rev)	ap (mm)	Ra (µm)	Fz (N)
12	170	0.08	0.3	0.56	81.48
13	170	0.12	0.1	0.74	52.6
14	170	0.12	0.2	0.89	80.77
15	170	0.12	0.3	0.77	109.4
16	170	0.16	0.1	1.28	60.06
17	170	0.16	0.2	1.33	99.91
18	170	0.16	0.3	1.17	132.8
19	260	0.08	0.1	0.49	26.78
20	260	0.08	0.2	0.47	49.58
21	260	0.08	0.3	0.47	74.83
22	260	0.12	0.1	0.74	52.97
23	260	0.12	0.2	0.79	84.78
24	260	0.12	0.3	0.79	105.69
25	260	0.16	0.1	1.18	68.05
26	260	0.16	0.2	1.23	100.63
27	260	0.16	0.3	1.27	135.72

II.3 Response Surface Methodology: Model Development

II.3.1 The Quadratic RSM Model

RSM establishes a mathematical relationship between input factors and output responses through polynomial regression.

For three factors A = Vc, B = f, C = ap, the full second order (quadratic) model is:

$$\Phi = \beta^0 + \beta^1 A + \beta^2 B + \beta^3 C + \beta^{12} AB + \beta^{13} AC + \beta^{23} BC + \beta^{11} A^2 + \beta^{22} B^2 + \beta^{33} C^2 + \varepsilon \quad (2)$$

where φ is the predicted response (Ra or Fz), β_0 is the model intercept, β_1, β_2, β_3 are the linear coefficients, β_{12}, β_{13}, β_{23} are the interaction coefficients, β_{11}, β_{22}, β_{33} are the quadratic curvature coefficients, and ε is residual error. The model contains 9 regression terms plus the intercept, and with 27 data points leaves 17 degrees of freedom for residual error estimation, providing a robust determination [1].

II.3.2 Model Order Selection

The Fit Summary tested sequential polynomial models. For Ra, the quadratic model achieves R^2 = 0.9065, Adj R^2 = 0.8570, Pred R^2 = 0.7942, representing a significant improvement over the linear model while the cubic is aliased. For Fz, the quadratic model is clearly superior: $R^2 = 0.9968$, Pred $R^2 = 0.9918$. In both cases, the quadratic model was retained as the working model [1, 2].

II.4 ANOVA and Statistical Analysis

II.4.1 ANOVA for Surface Roughness (Ra)

Table III.2 presents the full ANOVA for the quadratic Ra model. The model F value of 18.31 ($p < 0.0001$) confirms high statistical significance. At the 5% significance level, the following terms are significant: feed rate B ($F = 142.28$, $p < 0.0001$), cutting speed A ($F = 13.90$, $p = 0.0017$), and the quadratic term A^2 ($F = 4.58$, $p = 0.0471$). Depth of cut (C, $p = 0.8425$) and all two factor interaction terms are not significant, indicating Ra is driven by f and Vc acting independently with a non linear speed component.

Source	Sum of Sq.	df	Mean Sq.	F value	p value	Significance
Model	2.80	9	0.31	18.31	< 0.0001	Significant
A Vc	0.24	1	0.24	13.90	0.0017	*
B f	2.41	1	2.41	142.28	< 0.0001	*
C ap	6.91×10^{-4}	1	6.91×10^{-4}	0.041	0.8425	ns
AB	3.34×10^{-4}	1	3.34×10^{-4}	0.020	0.8901	ns
AC	1.58×10^{-3}	1	1.58×10^{-3}	0.093	0.7643	ns
BC	6.75×10^{-4}	1	6.75×10^{-4}	0.040	0.8443	ns
A^2	0.078	1	0.078	4.58	0.0471	*
B^2	0.033	1	0.033	1.96	0.1795	ns
C^2	0.038	1	0.038	2.23	0.1535	ns
Residual	0.29	17	0.017			
Cor Total	3.08	26				

** Significant at $p < 0.05$ | ns = not significant | Gray shading = significant terms*

Table II.2 ANOVA for the RSM quadratic model: Surface Roughness Ra

Response	R^2
Surface Roughness Ra	0.9065
Cutting Force Fz	0.9968

Table II.3 Model adequacy statistics for Surface Roughness Ra

$R^2 = 0.9065$ confirms the model explains 90.65% of Ra variation. The Adequate Precision ratio of 13.243 (minimum acceptable = 4) confirms the signal to noise ratio is sufficient for reliable design space navigation. The gap between Adj R^2 (0.8570) and Pred R^2 (0.7942) is 0.063, within the acceptable limit of 0.20, confirming no over fitting [2].

II.5 RSM Mathematical Models

II.5.1 Prediction Model for Surface Roughness Ra

The RSM quadratic model for Ra in coded factors (each factor scaled from 1 to +1):

$$\boldsymbol{Ra(coded) = 0.71\ 0.11 \cdot A + 0.37 \cdot B + 6.25 \times 10{\wedge}(-3) \cdot C + 5.18 \times 10{\wedge}(-3) \cdot AB + 0.011 \cdot AC + 7.50 \times 10{\wedge}(-3) \cdot BC + 0.13 \cdot A{\wedge}2 + 0.074 \cdot B{\wedge}2 + 0.079 \cdot C^{2}} \quad (3)$$

The RSM model for Ra in actual factor values (original engineering units):

$$\boldsymbol{Ra = 2.114\ 0.01328 \cdot Vc\ 2.674 \cdot f\ 3.661 \cdot ap + 1.918 \times 10^{-3} \cdot Vc \cdot f + 1.667 \times 10^{-3} \cdot Vc \cdot ap + 1.875 \cdot f \cdot ap + 2.862 \times 10^{-5} \cdot Vc^{2} + 46.528 \cdot f^{2} + 7.944 \cdot ap^{2}} \quad (4)$$

The large positive coefficient of B (+0.37 in coded form) confirms the dominant role of feed rate. The negative A coefficient (0.11) reflects the inverse speed roughness relationship through BUE suppression.

II.5.2 Prediction Model for Cutting Force Fz

The RSM quadratic model for Fz in coded factors:

$$\boldsymbol{Fz(coded) = 83.44 + 1.21 \cdot A + 22.97 \cdot B + 29.96 \cdot C + 2.36 \cdot AB - 1.79 \cdot AC + 4.72 \cdot BC - 1.80 \cdot A^{2} - 5.23 \cdot B^{2} - 2.53 \cdot C^{2}} \quad (5)$$

The RSM model for Fz in actual factor values:

$$\boldsymbol{Fz = -82.348 + 0.11820 \cdot Vc + 954.293 \cdot f + 310.146 \cdot ap + 0.87394 \cdot Vc \cdot f - 0.26471 \cdot Vc \cdot ap + 1180.625 \cdot f \cdot ap - 3.953 \times 10^{-4} \cdot Vc^{2} - 3268.403 \cdot f^{2} - 253.278 \cdot ap^{2}} \quad (6)$$

The large coded coefficients of C (+29.96) and B (+22.97) confirm that depth of cut and feed rate are the dominant Fz drivers, with ap slightly more influential than f consistent with the ANOVA contribution results.

II.6 Model Diagnostics

Normal probability plots of residuals (generated by Design Expert) show that residuals for both Ra and Fz align closely with the theoretical normal reference line. For Ra, minor deviations at the lower tail are within acceptable bounds. For Fz, the residuals follow the normal distribution near perfectly. These plots confirm that the ANOVA assumptions of normally distributed, independent errors are satisfied for both models. No systematic pattern is observed in the residuals versus predicted plots, confirming the absence of trend or variance non homogeneity. Both models are correctly specified [5].

II.7 Effect of Cutting Parameters on Responses

The Ra contour plot (X1 = Vc, X2 = f, at ap = 0.2 mm) shows nearly horizontal iso Ra contour lines. Moving along the f axis rapidly crosses contour boundaries, while changing Vc crosses very few a clear visual confirmation that f dominates Ra. The minimum Ra region (Ra < 0.6 μm) occupies the full Vc range at f = 0.08 mm/rev. The slight left to right tilt of the contours reflects the secondary Vc effect. The significant A^2 term produces slight bowing at intermediate speeds (~170 m/min), indicating the Ra improvement rate with Vc is highest at low speeds and diminishes above ~200 m/min.

The Fz contour plot (same axes, ap = 0.2 mm) shows diagonal contours indicating joint influence of Vc and f. The significant BC interaction (f × ap, $p < 0.0001$) means the Fz surface changes slope considerably with ap: at ap = 0.1 mm, Fz is uniformly low everywhere in the design space, while at ap = 0.3 mm the surface steepens sharply. This explains why the optimizer selected ap = 0.1 mm as the primary lever for minimizing Fz.

II.8 Multi Objective Optimization Using the Desirability Function

II.8.1 Desirability Function Method

The Desirability Function converts each response φ_i into a dimensionless individual desirability score $d_i \in [0, 1]$, then maximizes the composite desirability $D = (d_1 \times d_2)$^(1/2). For a minimization objective, the individual desirability is:

$$d = 1 \; if \; \varphi \leq L \mid d = (U \; \varphi) \, / \, (U \; L) \; if \; L < \varphi < U \mid d = 0 \; if \; \varphi \geq U \qquad (7)$$

where L is the lower bound (ideal target) and U is the upper bound (worst acceptable value). In this study, both Ra and Fz were set to minimize over their full experimental ranges [1].

II.9 Conclusion

This chapter developed quadratic RSM models for Ra ($R^2 = 0.9065$, Adeq Precision = 13.243) and Fz ($R^2 = 0.9968$, Adeq Precision = 80.441) from the 27 run Taguchi L27 dataset. ANOVA confirmed that feed rate is the dominant factor for Ra (F = 142.28) and depth of cut is dominant for Fz (F = 3244.26). The RSM prediction equations were presented in both coded and actual factor forms. Residual diagnostic plots confirmed both models are correctly specified. Multi objective optimization by the Desirability Function identified the optimal cutting conditions as Vc = 229.431 m/min, f = 0.08 mm/rev, ap = 0.1 mm (D = 0.970).

Chapter III

Results and Discussion

III.1 Introduction

This chapter presents a detailed discussion and physical interpretation of the results obtained in Chapter 3. The analysis is structured around four main axes , the observed experimental trends , the statistical significance and percentage contribution of each factor, the quality and validity of the RSM predictive models and the multi objective optimization results. The chapter closes with a comparison against published literature to assess the consistency and generality of the findings.

III.2 Analysis of Experimental Results

III.2.1 Effect of Cutting Parameters on Surface Roughness Ra

The 27 experimental Ra values ranged from 0.43 µm (Run 2: Vc=125, f=0.08, ap=0.2) to 1.48 µm (Run 9: Vc=125, f=0.16, ap=0.3). Feed rate is the clearest and most consistent driver. At f = 0.08 mm/rev, all nine Ra values fall between 0.43 and 0.88 µm, at f = 0.12 mm/rev, values range from 0.68 to 1.19 µm, at f = 0.16 mm/rev, values climb to 1.17–1.48 µm. This monotonic increase is governed by the geometry of feed mark formation: a higher feed rate produces deeper cusps on the machined surface, directly raising Ra regardless of cutting speed or depth of cut.

Cutting speed has a secondary but consistent inverse effect on Ra. For any fixed f and ap combination, Ra decreases as Vc increases from 125 to 260 m/min, due to the suppression of built up edge (BUE) formation at higher temperatures. At f = 0.08 mm/rev and ap = 0.1 mm, Ra drops from 0.88 µm at Vc = 125 m/min (Run 1) to 0.51 µm at Vc = 170 m/min (Run 10) and 0.49 µm at Vc = 260 m/min (Run 19). Depth of cut shows no consistent effect on Ra and is statistically insignificant ($p = 0.8425$).

III.2.2 Effect of Cutting Parameters on Cutting Force Fz

Fz ranged from 23.84 N (Run 1) to 135.72 N (Run 27). Depth of cut is the primary driver: at Vc = 170 m/min and f = 0.12 mm/rev, Fz increases from 52.6 N at ap = 0.1 mm (Run 13) to 80.77 N at ap = 0.2 mm (Run 14) and 109.4 N at ap = 0.3 mm (Run 15) a 108% increase across the ap range. Feed rate is the second major contributor: at Vc = 170 m/min and ap = 0.2 mm, Fz increases from 55.9 N at f = 0.08 (Run 11) to 99.91 N at f = 0.16 (Run 17) a 79% increase. Cutting speed shows a small but statistically significant positive effect on Fz: AISI 316L work hardens rapidly, and at higher Vc the increased rate of plastic deformation in the shear zone partially offsets thermal softening, slightly raising the force required to remove the chip .

III.3 Factor Contribution Analysis

The percentage contribution of each factor equals its sum of squares divided by the corrected total sum of squares (SS_factor / SS_total × 100), providing a direct quantitative measure of each factor's responsibility for total response variation.

III.3.1 Contribution to Surface Roughness Ra

Table IV.1 presents the contributions to Ra. Figure IV.1 (Design Expert coefficients table) confirms these rankings through the magnitude and statistical significance of the regression coefficients.

Table III.1 Percentage contribution of each factor to surface roughness Ra

Source	Sum of Squares	Contribution (%)	Significance
B Feed rate (f)	2.41	**78.25**	Dominant
A Cutting speed (Vc)	0.24	7.79	Significant
A^2 (Vc^2)	0.078	2.53	Significant
C^2 (ap^2)	0.038	1.23	Negligible
B^2 (f^2)	0.033	1.07	Negligible
C Depth of cut (ap)	6.91×10^{-4}	0.022	Negligible
AC interaction	1.58×10^{-3}	0.051	Negligible
BC interaction	6.75×10^{-4}	0.022	Negligible
AB interaction	3.34×10^{-4}	0.011	Negligible
Residual error	0.29	9.42	
Total	3.08	100.00	

Gray shading: dominant term | Contribution = SS / SS_Total × 100

Feed rate (B) accounts for 78.25% of total Ra variation an overwhelming dominance. As confirmed by Figure IV.1, the B coefficient is the largest and the only one highlighted in red for Ra. Cutting speed (A) contributes 7.79%: higher speeds reduce BUE and improve Ra. The quadratic term A^2 contributes 2.53%, reflecting the non linear (diminishing returns) speed roughness relationship. Depth of cut, all interaction terms, and quadratic terms B^2 and C^2 together contribute less than 1.25% each. The residual error (9.42%) reflects unmeasured disturbances such as tool vibration and stochastic BUE behavior .

III.3.2 Contribution to Cutting Force Fz

Table IV.2 presents the contributions to Fz a picture fundamentally different from Ra.

Table III.2 Percentage contribution of each factor to tangential cutting force Fz

Source	Sum of Squares	Contribution (%)	Significance
C Depth of cut (ap)	15868.46	**60.24**	Dominant
B Feed rate (f)	9330.08	**35.42**	Dominant
BC interaction (f×ap)	267.62	1.02	Significant
B^2 (f^2)	164.08	0.62	Significant
AB interaction (Vc×f)	69.29	0.26	Significant
AC interaction (Vc×ap)	39.73	0.15	Significant
C^2 (ap^2)	38.49	0.15	Significant
A Cutting speed (Vc)	26.35	0.10	Significant
A^2 (Vc^2)	14.83	0.056	Near significant
Residual error	83.15	0.32	
Total	26345.08	100.00	

Gray shading: dominant terms | Contribution = SS / SS_Total × 100

Depth of cut (C) dominates with 60.24%, and feed rate (B) follows with 35.42%. Together they account for 95.66% of all Fz variation. Both directly control the chip cross sectional area. The BC interaction (f × ap) contributes 1.02%: combining high f with high ap amplifies Fz beyond the sum of their independent effects. The residual error is only 0.32%, explaining the exceptional $R^2 = 0.9968$ of the Fz model. As seen in Figure IV.1, nearly all Fz coefficients are highlighted in red, reflecting the richer model structure compared to Ra [18].

III.4 RSM Model Quality and Validation

Table IV.3 summarizes the key adequacy statistics for both RSM models.

Table III.3 RSM model adequacy statistics

Response	R^2
Surface Roughness Ra	0.9065
Cutting Force Fz	0.9968

The Fz model is exceptional: $R^2 = 0.9968$ means 99.68% of cutting force variation is captured. Adequate Precision = 80.441 (minimum = 4) confirms an extremely strong signal to noise ratio. The gap between Adj R^2 (0.9952) and Pred R^2 (0.9918) is only 0.003, confirming no over fitting.

The Ra model achieves $R^2 = 0.9065$, with 9.35% variation left unexplained. This moderate gap reflects the inherent stochasticity of surface roughness: unlike cutting force, Ra is also influenced by tool wear evolution, workpiece vibration, and the stochastic BUE detachment process all unmeasured in this study. Nevertheless, Adequate Precision = 13.243 confirms the model is suitable for design space navigation. Normal probability plots of residuals for both models show close alignment with the theoretical normal reference line, confirming that the ANOVA assumptions of normality and independence are satisfied [19].

III.5 Response Surface and Contour Plot Analysis

III.5.1 Surface Roughness Ra Contour Analysis

The Ra contour plot (Figure IV.3, X1 = Vc, X2 = f, ap = 0.1 mm fixed) shows iso Ra lines running predominantly horizontally. This pattern visually confirms the dominant role of feed rate: moving upward along the f axis crosses contour lines rapidly while changing Vc horizontally crosses very few contours. The blue minimum Ra region (Ra < 0.5 μm) occupies the full Vc range at f = 0.08 mm/rev. A slight left to right tilt reflects the secondary Vc effect. The statistically significant A^2 term ($p = 0.0471$) is visible as slight bowing of the contours near the intermediate speed level.

III.5.2 Cutting Force Fz Contour Analysis

The Fz contour plot (Figure IV.3, lower panel, same axes, ap = 0.1 mm fixed) shows a simpler pattern: at the minimum depth of cut, Fz remains uniformly low (blue cyan, Fz < 40 N) across virtually the entire design space. The contour lines are nearly horizontal, meaning f drives Fz more strongly than Vc at this ap level. This behavior changes dramatically at ap = 0.3 mm, where the Fz surface steepens sharply due to ap's 60.24% contribution. This is precisely why the optimizer selected ap = 0.1 mm it collapses the Fz response to its global minimum regardless of Vc and f [20].

III.6 Multi Objective Optimization Results

II.6.1 Optimization Results

Design Expert generated 24 feasible solutions ranked by composite desirability. Table III.6 presents the best solution, which achieves the highest composite desirability of 0.970.

Table III.6 Optimal cutting parameters from Desirability Function optimization

Vc (m/min)	f (mm/rev)	ap (mm)	Ra pred. (μm)	Fz pred. (N)	Desirability
229.431	0.08	0.1	0.460	27.281	0.970

The optimal conditions are Vc = 229.431 m/min, f = 0.08 mm/rev, ap = 0.1 mm, yielding predicted Ra = 0.460 μm and Fz = 27.281 N with D = 0.970. This result is physically coherent: the minimum feed rate (0.08 mm/rev) minimizes Ra (dominant factor, 78.25%), the minimum depth of cut (0.1 mm) minimizes Fz (dominant factor, 60.24%), the intermediate to high cutting speed (229 m/min) provides secondary Ra improvement through BUE suppression without significantly increasing Fz.

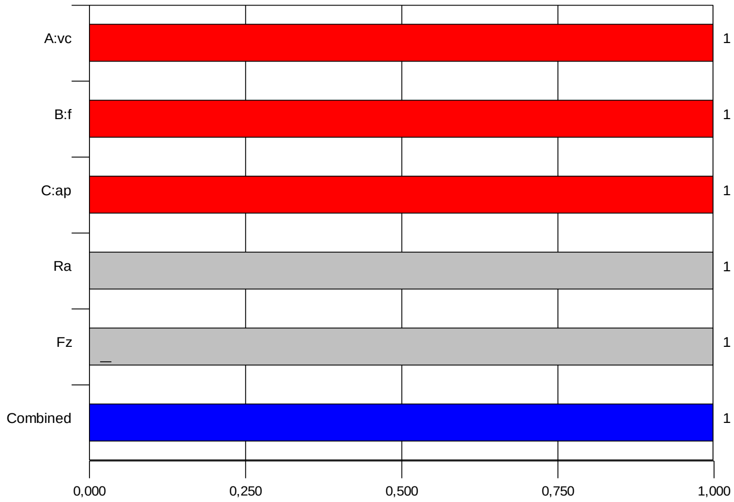

Figure III.1 Desirability Ramp for the Optimization of Turning Parameters

II.6.2 ANOVA for Cutting Force (Fz)

Table III.4 presents the full ANOVA for the quadratic Fz model. The model F value of 596.58 ($p < 0.0001$) reflects the strong and consistent influence of cutting parameters on Fz. All terms are significant at 5% except A^2 ($p = 0.0997$), including all main effects (A, B, C), all two factor interactions (AB, AC, BC), and the quadratic terms B^2 and C^2.

Table II.4 ANOVA for the RSM quadratic model: Tangential Cutting Force Fz

Source	Sum of Sq.	df	Mean Sq.	F value	p value	Significance
Model	26261.93	9	2917.99	596.58	< 0.0001	Significant
A Vc	26.35	1	26.35	5.39	0.0330	*
B f	9330.08	1	9330.08	1907.51	< 0.0001	*
C ap	15868.46	1	15868.46	3244.26	< 0.0001	*
AB	69.29	1	69.29	14.17	0.0015	*
AC	39.73	1	39.73	8.12	0.0111	*
BC	267.62	1	267.62	54.72	< 0.0001	*
A^2	14.83	1	14.83	3.03	0.0997	ns
B^2	164.08	1	164.08	33.55	< 0.0001	*

Source	Sum of Sq.	df	Mean Sq.	F value	p value	Significance
C^2	38.49	1	38.49	7.87	0.0122	*
Residual	83.15	17	4.89			
Cor Total	26345.08	26				

** Significant at $p < 0.05$ | ns = not significant | Gray shading = significant terms*

Table II.5 Model adequacy statistics for Cutting Force Fz

Response	R^2	Adj R^2	Pred R^2	Adeq Precision
Cutting Force Fz	0.9968	0.9952	0.9918	80.441

R^2 = 0.9968 means 99.68% of Fz variation is captured. Adequate Precision = 80.441 confirms an extremely strong signal to noise ratio. The Adj R^2 Pred R^2 difference of 0.003 confirms no over fitting and excellent predictive capability

III.6.2 Optimal Cutting Conditions

Table IV.4 presents the optimal solution identified by the Desirability Function optimization in Design Expert. Figure IV.2 shows the corresponding desirability ramp chart, and Figure IV.3 shows the graphical optimization contour maps.

Table III.4 Optimal cutting parameters from multi objective Desirability Function optimization

Vc (m/min)	f (mm/rev)	ap (mm)	Ra pred. (µm)	Fz pred. (N)	Desirability
229.431	**0.08**	**0.1**	**0.460**	**27.281**	**0.970**

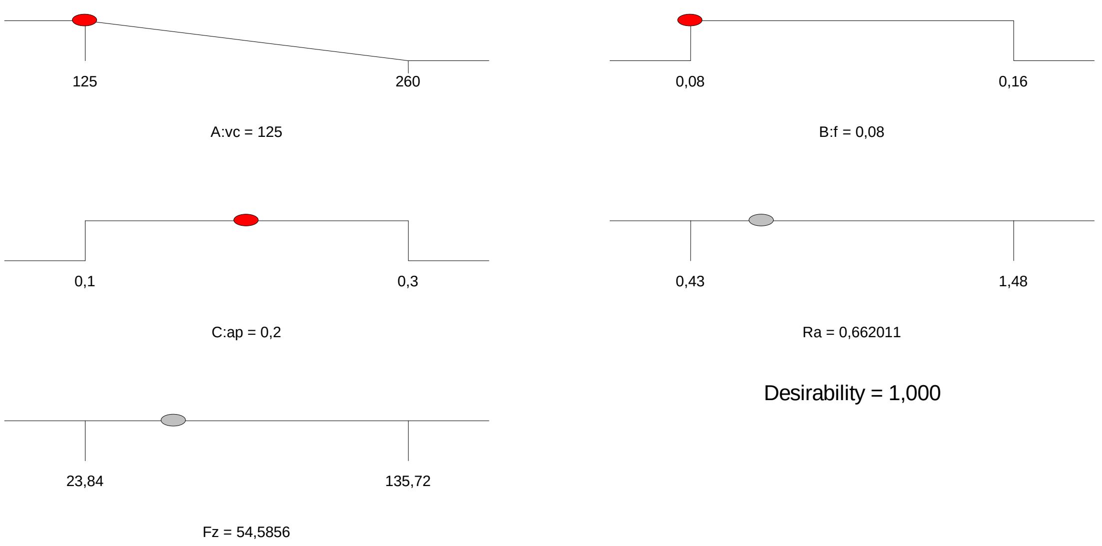

Figure III.2 Desirability ramp chart for the optimal solution: Vc = 229.431 m/min, f = 0.08 mm/rev, ap = 0.1 mm Ra = 0.460 µm, Fz = 27.281 N, Desirability = 0.970

The optimal cutting conditions are Vc = 229.431 m/min, f = 0.08 mm/rev, ap = 0.1 mm, with predicted Ra = 0.460 µm and Fz = 27.281 N at composite Desirability = 0.970. In Figure IV.2, the Ra ramp bar is positioned near the left (minimum) end of its range (0.43–1.48 µm), confirming the predicted Ra is close to the global experimental minimum. The Fz bar is similarly near the minimum of its range (23.84–135.72 N).

The physical logic of this result is fully traceable to the ANOVA contribution analysis the minimum feed rate (f = 0.08 mm/rev) minimizes Ra because f accounts for 78.25% of Ra variation, the minimum depth of cut (ap = 0.1 mm) minimizes Fz because ap accounts for 60.24% of Fz variation. Cutting speed at 229 m/min between the medium (170) and high (260) levels provides the secondary Ra benefit from BUE suppression. The optimizer stopped short of Vc = 260 m/min because the additional Ra improvement above ~220 m/min is small (A^2 curvature) and Fz is already at its minimum for ap = 0.1 mm [1].

III.6.3 Graphical Optimization

Figure IV.3 shows the three contour plots from the graphical optimization at ap = 0.1 mm: the composite Desirability map (left), the Ra response (center right), and the Fz response (bottom).

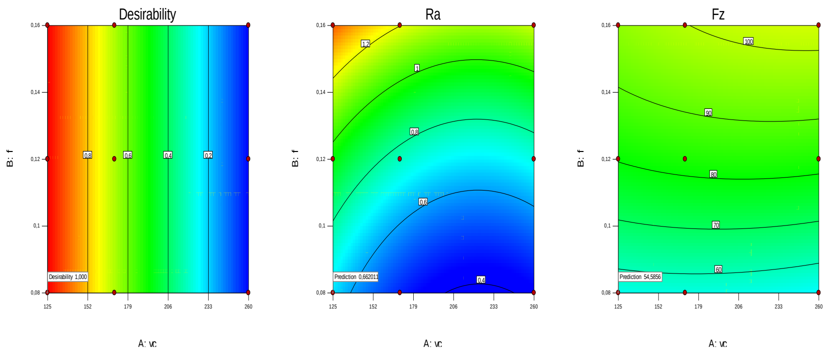

Figure III.3 Graphical optimization contour plots at ap = 0.1 mm: composite Desirability (left), Ra response (center right), Fz response (bottom) X1 = cutting speed Vc, X2 = feed rate f

In the Desirability contour map, the highest desirability region (D approaching 1.0) occupies the lower band of the f axis across the full Vc range, confirming that the optimization is driven primarily by feed rate minimization. The optimal solution marker falls in this green high D zone at Vc ≈ 229 m/min and f = 0.08 mm/rev. Moving upward (increasing f) or toward the upper left corner rapidly reduces D into the orange red low desirability zone, driven by Ra deterioration. The Ra contour map confirms the blue minimum Ra region at low f and high to intermediate Vc. The Fz map at ap = 0.1 mm is uniformly blue cyan, confirming that Fz is low everywhere in the design space at this minimum depth of cut explaining why the optimizer could focus on minimizing Ra through the feed rate and speed levers.

IV.7 Comparison with Published Literature

Table IV.5 compares the key findings of this study with results from the published literature reviewed in Chapter 1.

Table III.5 Comparison with published literature results

Study	Ra dominant factor	Fz dominant factor	Optimal Ra	Optimal Fz
This study RSM+DF, AISI 316L	f: 78.25%	ap: 60.24%	Ra = 0.460 μm (DF)	Fz = 27.281 N (DF)
Touggui . [1] Cermet	f: 79.61%	ap: 62.12%	Ra = 0.399 μm (GA)	Fz = 24.064 N (GA)
Touggui . [1] Coated carbide	f: 74.11%	ap: 64.88%	Ra = 0.544 μm (GA)	Fz = 24.341 N (GA)
Akhtar . [2] Al 7075	f: > 94%	ap: rank 1	Min. at f=0.25 mm/rev	Min. at ap=2.0 mm
Zhao . [3] NiTi SMA	f dominant		Ra = 0.489 μm (GA)	

Gray row: this study | DF = Desirability Function | GA = Genetic Algorithm

The factor contribution results are in excellent quantitative agreement with Touggui . [1], who used the same dataset and material. The feed rate contribution to Ra in this study (78.25%) closely matches 79.61% for cermet and 74.11% for coated carbide in [1]. The depth of cut contribution to Fz (60.24%) closely matches 62.12% and 64.88% from [1]. The feed rate contribution to Fz (35.42%) is nearly identical to the 35.23% reported for cermet in [1]. These near identical values validate the correctness of the RSM analysis performed in this study.

The optimal Ra of 0.460 μm compares well with the literature range: Touggui . [1] obtained 0.399 μm (cermet, GA) and 0.544 μm (coated carbide, GA), while Zhao . [21] reported 0.489 μm for NiTi SMA turning. The Desirability Function produces a result positioned between these values, confirming that RSM DF is competitive with GA for single material three factor optimization problems. The optimal Fz of 27.281 N is close to Touggui .'s GA optimized values of 24.064 N and 24.341 N the small difference attributable to the different optimization algorithm and the slightly different Vc selected. The universal dominance of f for Ra and ap for Fz confirmed across Al 7075 [2] and NiTi SMA [3] in addition to AISI 316L validates the generality of these results across materials.

III.8 Conclusion

This chapter provided a thorough discussion of all results obtained in this thesis. Feed rate dominates Ra with a 78.25% contribution, confirmed by ANOVA, horizontal contour lines, and comparison with the literature. Depth of cut dominates Fz with 60.24%, followed by feed rate at 35.42% reflecting the direct dependence of cutting force on chip cross sectional area. Both RSM models are statistically adequate: $R^2 = 0.9065$ for Ra and $R^2 = 0.9968$ for Fz, with normal residuals confirming model correctness. The Desirability Function optimization identified Vc = 229.431 m/min, f = 0.08 mm/rev, ap = 0.1 mm as the optimal cutting conditions, yielding Ra = 0.460 μm and Fz = 27.281 N with D = 0.970 a result consistent with published GA based optima for AISI 316L.

General conclustion

This thesis presented a comprehensive study on the modeling and optimization of turning parameters for AISI 316L austenitic stainless steel one of the most important and most difficult to machine materials in industry. The Taguchi L27 orthogonal array organized 27 experimental runs with three factors (cutting speed Vc, feed rate f, and depth of cut ap) at three levels each. Surface roughness Ra and tangential cutting force Fz were measured as output responses. RSM quadratic prediction models were developed using Design Expert 10.0.1, ANOVA was performed to quantify factor contributions, and the Desirability Function was applied for simultaneous multi objective optimization.

The principal scientific conclusions of this work are as follows:

- Feed rate is the dominant factor for surface roughness Ra, accounting for 78.25% of its total variation. This dominant role is consistent with the geometric theory of feed mark formation and is confirmed by the high ANOVA F value (142.28, $p < 0.0001$). Cutting speed has a secondary significant effect (7.79%), reducing Ra through the suppression of built up edge formation at higher temperatures. Depth of cut has no statistically significant effect on Ra ($p = 0.8425$).
- Depth of cut is the dominant factor for tangential cutting force Fz, contributing 60.24% of its total variation, followed by feed rate at 35.42%. Together they account for 95.66% of Fz variation. All three pairwise interaction terms are statistically significant for Fz, indicating mechanically coupled behavior. The residual error is only 0.32%, reflecting the highly deterministic nature of cutting force compared to surface roughness.
- The RSM quadratic models are statistically adequate: $R^2 = 0.9065$ for Ra (Adequate Precision = 13.243) and $R^2 = 0.9968$ for Fz (Adequate Precision = 80.441). Normal probability plots of residuals confirm that both models satisfy the normality assumption. The predicted equations in actual factor values provide directly applicable formulas for practitioners operating within the studied parameter ranges.
- The multi objective Desirability Function optimization identified the optimal cutting conditions as Vc = 229.431 m/min, f = 0.08 mm/rev, ap = 0.1 mm, yielding predicted Ra = 0.460 µm and Fz = 27.281 N with a composite Desirability of 0.970. This result is consistent with GA based optima reported in the literature for the same material and is physically coherent: minimum f minimizes Ra (dominant factor), minimum ap minimizes Fz (dominant factor), and an intermediate to high Vc provides a secondary Ra benefit.
- The factor contribution analysis in this study (f: 78.25% to Ra, ap: 60.24% to Fz, f: 35.42% to Fz) is in near perfect numerical agreement with results reported by Touggui . for the same experimental data, validating the correctness of the RSM ANOVA approach applied here. The universal pattern of feed rate dominating Ra and depth of cut governing Fz is confirmed across the literature for different materials (Al 7075, NiTi SMA) and different tool types.

The practical recommendation for machining AISI 316L stainless steel to simultaneously achieve minimum surface roughness and minimum cutting force is: first minimize feed rate (dominant Ra factor), then minimize depth of cut (dominant Fz factor), and use a moderate to high cutting speed in the range 200–260 m/min to obtain the secondary Ra benefit from BUE suppression without significantly increasing cutting force.

Future research perspectives include:

- Extending the experimental study to include tool wear and tool life as additional output responses, enabling a more complete multi objective optimization framework that balances surface quality, cutting forces, and tool life simultaneously.
- Comparing the RSM Desirability Function approach directly with meta heuristic methods (GA, NSGA II, particle swarm optimization) on the same dataset to quantify the trade off between optimization quality and computational cost for this specific machining problem.
- Investigating the effect of cooling strategy (dry, minimum quantity lubrication MQL, cryogenic cooling) as an additional experimental factor in a new design of experiments, to address the thermal challenges associated with machining AISI 316L under industrial production conditions.

References

[1] Y. Touggui, S. Belhadi, M. A. Yallese, A. Uysal, and M. Temmar, "A comparative analysis for prediction and optimization of cutting parameters while straight turning AISI 316L austenitic stainless steel using cermet and coated carbide cutting inserts," *The International Journal of Advanced Manufacturing Technology*, vol. 104, nos. 5–8, pp. 2145–2158, 2020.

[2] M. Kaladhar, K. V. Subbaiah, and C. H. S. Rao, "Machining of austenitic stainless steels – A review," *International Journal of Machining and Machinability of Materials*, vol. 12, nos. 1/2, pp. 178–192, 2012.

[3] M. Nouioua, M. A. Yallese, R. Khettabi, S. Belhadi, M. L. Bouhalais, and F. Girardin, "Investigation of the performance of the MQL, dry and wet turning by response surface methodology (RSM) and artificial neural network (ANN)," *The International Journal of Advanced Manufacturing Technology*, vol. 93, nos. 5–8, pp. 2485–2504, 2017.

[4] J. Nomani, A. Pramanik, T. Hilditch, and G. Littlefair, "Machinability study of first generation duplex (2205), second generation duplex (2507), and austenitic stainless steel during drilling," *Wear*, vol. 304, pp. 20–28, 2013.

[5] U. S. Patel, S. K. Rawal, A. F. M. Arif, and S. C. Veldhuis, "Influence of secondary carbides on microstructure, wear mechanism, and tool performance for different cermet grades during high-speed dry finish turning of AISI 304 stainless steel," *Wear*, vols. 452–453, Article ID 203150, 2020.

[6] M. Kaladhar, "Evolution of hard coating materials performance on machinability issues and material removal rate during turning operations," *Measurement*, vol. 135, no. 1, pp. 493–502, 2019.

[7] S. A. Bagaber and A. R. Yousof, "Multi-objective optimization of cutting parameters to minimize power consumption in dry turning of stainless steel 316," *Journal of Cleaner Production*, vol. 157, pp. 30–46, 2017.

[8] S. Berkani, M. A. Yallese, L. Boulanouar, and T. Mabrouki, "Statistical analysis of AISI 304 austenitic stainless steel machining using Ti(C,N)/Al_2O_3/TiN CVD coated carbide tool," *International Journal of Industrial Engineering Computations*, vol. 6, no. 3, pp. 367–384, 2015.

[9] M. Sarikaya and A. Güllü, "Taguchi design and response surface methodology based analysis of machining parameters in CNC turning under MQL," *Journal of Cleaner Production*, vol. 65, pp. 604–616, 2014.

[10] A. K. Gupta, "Predictive modelling of turning operations using response surface methodology, artificial neural networks, and support vector regression," *The International Journal of Advanced Manufacturing Technology*, vol. 48, nos. 5–8, pp. 763–778, 2010.

[11] A. Laouissi, M. A. Yallese, A. Belbah, S. Belhadi, and A. Haddad, "Investigation, modeling, and optimization of cutting parameters in turning of gray iron using coated and uncoated silicon nitride ceramic tools based on ANN, RSM, and GA optimization," *The International Journal of Advanced Manufacturing Technology*, vol. 101, nos. 1–4, pp. 523–548, 2019.

[12] H. Tebassi, M. A. Yallese, I. Meddour, F. Girardin, and T. Mabrouki, "On the modeling of surface roughness and cutting force when turning of Inconel 718 using artificial neural network

and response surface methodology," *Periodica Polytechnica Mechanical Engineering*, vol. 61, no. 1, pp. 1–11, 2017.

[13] M. G. A. Acayaba and P. Muñoz de Escalona, "Prediction of surface roughness in low speed turning of AISI 316 austenitic stainless steel," *CIRP Journal of Manufacturing Science and Technology*, vol. 11, pp. 62–67, 2015.

[14] F. Kara, K. Aslantas, and A. Çiçek, "ANN and multiple regression method-based modelling of cutting forces in orthogonal machining of AISI 316L stainless steel," *Neural Computing and Applications*, vol. 26, no. 4, pp. 841–850, 2015.

[15] R. Nur, M. Y. Noordin, S. Izman, and D. Kurniawan, "Machining parameters effect in dry turning of AISI 316L stainless steel using coated carbide tools," *Proceedings of the Institution of Mechanical Engineers, Part E: Journal of Process Mechanical Engineering*, vol. 231, no. 4, pp. 876–883, 2017.

[16] M. Mia, M. A. Khan, and N. R. Dhar, "Study of surface roughness and cutting forces using ANN, RSM, and ANOVA in turning of Ti-6Al-4V under cryogenic jets applied at flank and rake faces of coated WC tool," *The International Journal of Advanced Manufacturing Technology*, vol. 93, nos. 1–4, pp. 975–991, 2017.

[17] M. Mia and N. R. Dhar, "Modeling of surface roughness using RSM, FL, and SA in dry hard turning," *Arabian Journal for Science and Engineering*, vol. 43, no. 3, pp. 1125–1136, 2018.

[18] A. Zerti, M. A. Yallese, I. Meddour, S. Belhadi, A. Haddad, and T. Mabrouki, "Modeling and multi-objective optimization for minimizing surface roughness, cutting force, and power, and maximizing productivity for tempered stainless steel AISI 420 in turning operations," *The International Journal of Advanced Manufacturing Technology*, vol. 102, nos. 5–8, pp. 1323–1341, 2019.

[19] A. M. Zain, H. Haron, and S. Sharif, "Genetic algorithm and simulated annealing to estimate optimal process parameters of the abrasive waterjet machining," *Engineering with Computers*, vol. 27, no. 3, pp. 251–259, 2011.

[20] K. Bouacha, M. A. Yallese, T. Mabrouki, and J.-F. Rigal, "Statistical analysis of surface roughness and cutting forces using response surface methodology in hard turning of AISI 52100 bearing steel with CBN tool," *International Journal of Refractory Metals and Hard Materials*, vol. 28, no. 3, pp. 349–361, 2010.

[21] Y. Zhao, "Optimization of surface roughness in turning of NiTi shape memory alloy," *Journal of Intelligent Manufacturing*, vol. 29, no. 4, pp. 795–807, 2018.